Proc. 24th Chinese Control and Decision Conference
pp. 3528-3533, Taiyuan, China, (2012)

Feedforward Control for Disturbance Rejection: Model Matching and Other Methods

Hua Zhong[1], Lucy Pao[2], Raymond de Callafon[3]

1. University of Colorado Boulder, Boulder, CO 80302, USA
E-mail: zhongh@colorado.edu

2. University of Colorado Boulder, Boulder, CO 80302, USA
E-mail: pao@colorado.edu

3. University of California at San Diego, La Jolla, CA 92093, USA
E-mail: callafon@ucsd.edu

Abstract: Feedforward control can improve disturbance rejection performance of a system when the measurement of the disturbance is available. This paper discusses the design of feedforward control in the discrete-time domain using the model matching methods that compute optimal and stable feedforward controllers. It is shown that the existence of a non-zero solution to the model matching problem depends on the difference between the relative degrees of the plant dynamics and the disturbance dynamics. A number of approximate dynamic inversion techniques commonly used for feedforward control design are reviewed and compared with the model matching methods. These feedforward control design methods are then applied to the application of an example tape head track-following servo system where the feedforward controller aims at reducing the position error caused by the lateral tape motion. Simulation results are presented to demonstrate the effectiveness of the feedforward control.

Key Words: Feedforward Control, Model Matching, Tape Storage

1 INTRODUCTION

Feedforward control can improve disturbance rejection performance of a system when disturbance measurements are available. As show in Figure 1, the transfer function T_{ed} from the disturbance d to the output error e is given by

$$T_{ed} = F + GC_{ff}. \tag{1}$$

where G and F represent the dynamics of the plant and the disturbance, respectively. The feedforward controller C_{ff} aims to minimize the impact from d on e, possibly over a desired frequency range. Without loss of generality, the plant G is assumed to be stable as a feedback controller could be added for stabilization otherwise.

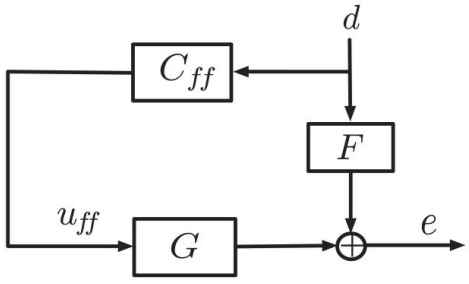

Figure 1: The feedforward controller C_{ff} aims to attenuate the effects from the disturbance d on the output error e.

This work was partly supported by the Information Storage Industry Consortium (INSIC) and Oracle Corporation. We are also grateful for support from Professor Sinan Müftü of Northeastern University in Boston, MA for providing us with tape simulation data.

One typical design of the feedforward control is to approximate the inverse of G and compute a stable and causal approximation of $-G^{-1}F$. Dynamic inversion and approximate dynamic inversion techniques have been widely studied to design the feedforward controller C_{ff}. Commonly used methods include the zero phase error tracking control (ZPETC) [11], the zero magnitude error tracking control (ZMETC) [10] (and references therein), and the non-causal Taylor series approximation method [8].

As an alternative to dynamic inversion, H_2 and H_∞ model matching methods can be used to find an optimal feedforward controller C_{ff} that minimizes the norm of the transfer function T_{ed} [3] [4]. A generic set of tools to solve H_2 or H_∞ preview control problems has been summarized in [5]. In this paper, we investigate the H_2 model matching method for disturbance rejection in the discrete-time domain. The existence of the solution for such a problem depends on the difference between the relative degrees of the plant dynamics G and the disturbance dynamics F. We derive the requirements on plant dynamics and disturbance dynamics such that the model matching problem has a non-zero solution. Computing optimal controller by minimizing a norm on the transfer function T_{ed} may lead to large control signal u_{ff} if no penalty is imposed on the norm of C_{ff}. This can be solved by augmenting the model matching techniques with a simultaneous minimization of a (weighted form) of C_{ff} to provide a trade-off between minimizing e and the control signal u_{ff}.

In this paper, a few approximate dynamic inversion techniques are reviewed and compared with the augmented

978-1-4577-2074-1/12/$26.00

model matching method. These controller design methods are then applied to the application of an example tape head track-following servo system where the feedforward controller is designed to reduce the position error caused by lateral tape motion. The remainder of the paper is organized as follows. Section 2 discusses the requirements on the plant dynamics G and the disturbance dynamics F for the H_2 model matching method to yield non-zero solutions. We then review the approximate dynamic inversion techniques in Section 3. To demonstrate the effectiveness of the feedforward control, we present the simulation results of implementing the feedforward control design on the example tape head track-following servo system in Section 4. Finally, Section 5 provides conclusions and discussion.

2 MODEL MATCHING METHODS

2.1 Problem Formulation

To minimize the variance of the output error e due to the disturbance d (Figure 1) in the discrete-time domain, the model matching methods compute a feedforward controller $C_{ff}(z)$ such that either the H_2 or H_∞ norm on the transfer function $T_{ed}(z)$ is minimized [3], [4], [5]. In this paper, we restrict ourselves to minimize the H_2 norm of the transfer function $T_{ed}(z)$, as described in the following equation

$$C_{ff}(z)=\arg\min_{C_{ff}(z)\in R\mathcal{H}_\infty}\|[F(z)+G(z)C_{ff}(z)]D_d(z)\|_2. \quad (2)$$

Here, the discrete-time filter $D_d(z)$ is stable and stably invertible. Moreover, $|D_d(e^{j\omega})|^2=\Phi_d(\omega)$, where $\Phi_d(\omega)$ is the spectral factorization of the spectrum of the disturbance signal d. Without loss of generality, we set $D_d(z)=I$ to simplify the formula and discussion. It should be noted that $C_{ff}(z)$ is required to be stable ($\in R\mathcal{H}_\infty$) and we allow $C_{ff}(z)$ to be proper. The discrete-time variable z is omitted in some of the equations in this paper to save space.

2.2 Direct Solution for Minimum-Phase (MP) Systems

Analytically, if $G(z)$ only has minimum-phase (MP) zeros and is exactly proper, $G(z)$ is invertible and the feedforward controller can be computed directly via

$$C_{ff}(z)=-G^{-1}(z)F(z). \quad (3)$$

When $G(z)$ only has MP zeros and is strictly proper, the inverse $G^{-1}(z)$ is stable but non-causal. Denote the relative degrees of $G(z)$ and $F(z)$ as r_G and r_F, respectively, we can write $G(z)=G(z)z^{r_G}z^{-r_G}=\bar{G}(z)z^{-r_G}$, where $\bar{G}(z)=G(z)z^{r_G}$ is invertible. Following (3), the feedforward controller is

$$C_{ff}(z)=-\bar{G}^{-1}(z)F(z)z^{r_G}$$

and $C_{ff}(z)$ is proper iff $F(z)z^{r_G}$ is proper, that is, the relative degree of $F(z)$ is greater or equal to that of $G(z)$.

When $r_F\geq r_G$, the disturbance can be completely rejected for a MP system $G(z)$ as $T_{ed}(z)=0$. In the special case of $r_G=0$, the direct solution of the $C_{ff}(z)$ is given in (3). When $r_F<r_G$, only the zero solution $C_{ff}(z)=0$ should be used, as a non-zero $C_{ff}(z)$ will worsen the variance of the error signal e. This effect will be explained in more detail when we examine the conditions for non-zero solutions.

2.3 Non-zero Solutions

When $G(z)$ has zeros outside the unit circle, the inverse $G^{-1}(z)$ is unstable and possibly non-causal. Approximate dynamic inversion techniques can be used to compute the approximate inversion $\tilde{G}^{-1}(z)$ of $G(z)$ and $C_{ff}(z)=-\tilde{G}^{-1}(z)F(z)$. However, whether the resulting feedforward controller $C_{ff}(z)$ would reduce the norm of $T_{ed}(z)$ is not clear.

Improving the disturbance rejection performance of a system by adding feedforward control is directly addressed in the model matching problem formulation in (2), provided a non-zero solution $C_{ff}(z)$ exists. To characterize when such a non-zero solution can be computed, we write the transfer function $T_{ed}(z)$ in (1) in a lower Linear Fractional Transformation (LFT) formulation

$$T_{ed}=\mathcal{F}_l(P,-C_{ff})=P_{11}-P_{12}C_{ff}(I+P_{22}C_{ff})^{-1}P_{21}, \quad (4)$$

where

$$P=\begin{bmatrix}P_{11}&P_{12}\\P_{21}&P_{22}\end{bmatrix}=\begin{bmatrix}F&G\\-I&0\end{bmatrix}.$$

With the state-space model of the LFT plant P given by

$$P\hat{=}\begin{bmatrix}A&B_1&B_2\\C_1&D_{11}&D_{12}\\C_2&D_{21}&0\end{bmatrix} \quad (5)$$

we have a properly specified discrete-time H_2 model matching problem with the optimality property summarized in the following lemma.

Lemma 1. *Let G be stable and exactly proper with a non-zero feedthrough matrix D_G ($D_G^{\mathrm{T}}D_G>0$). Let F be stable and (strictly) proper. Then*

$$\min_{C_{ff}(z)\in R\mathcal{H}_\infty}\|F(z)+G(z)C_{ff}(z)\|_2<\|F(z)\|_2$$

Proof. For the minimization of $\|\mathcal{F}_l(P,-C_{ff})\|_2$ over C_{ff} using the LFT representation (4) of P given in (5), we have the following four standard conditions to compute an optimal solution [4]:

1. (A,B_2) is stabilizable and (C_2,A) is detectable;
2. $\begin{bmatrix}A-j\omega I&B_2\\C_1&D_{12}\end{bmatrix}$ has full column rank for all ω;
3. $\begin{bmatrix}A-j\omega I&B_1\\C_2&D_{21}\end{bmatrix}$ has full row rank for all ω;
4. $D_{12}^{\mathrm{T}}D_{12}>0$ and $D_{21}D_{21}^{\mathrm{T}}>0$.

The first condition is for the stabilization via output feedback. Since both G and F are stable, this condition is satisfied. The second and third conditions are to guarantee that a solution can be computed via two Riccati equations [4]. Finally, the last condition guarantees that the proposed H_2 control problem is nonsingular. With the definition of P in (5), we see that $D_{21}=-I$ and $D_{21}D_{21}^{\mathrm{T}}>0$. Furthermore, $D_{12}^{\mathrm{T}}D_{12}>0$ is satisfied as G is exactly proper

and has a non-zero feedthrough matrix D_G. Hence, we have a properly specified discrete-time H_2 model matching problem that computes a non-zero solution of C_{ff}. With $C_{ff}(z) \neq 0$, we must have $\|F + GC_{ff}\|_2 < \|F\|_2$ as $\|F + GC_{ff}\|_2 = \|F\|_2$ only if $C_{ff}(z) = 0$. It should be noted that D_{11} does not play a role in computing the optimal solution of the model matching problem. □

The result in Lemma 1 states that a well-posed model matching problem can yield an optimal feedforward controller that reduces the H_2 norm of $T_{ed}(z)$. The well-posedness of the problem is directly related to the feedthrough matrix D_G of the exactly proper plant G. The result can be easily extended to a system $G(z)$ with a relative degree $r_G \geq 0$.

Theorem 1. *Let G and F be stable. Let G have a relative degree $r_G \geq 0$. If $r_F \geq r_G$, then*

$$\min_{C_{ff}(z)\in R\mathcal{H}_\infty} \|F(z) + G(z)C_{ff}(z)\|_2 < \|F(z)\|_2.$$

Proof. Define $\bar{G}(z) = G(z)z^{r_G}$, $\bar{G}(z)$ is then exactly proper with a non-zero feedthrough matrix D_G and $D_G^{\mathrm{T}} D_G > 0$. Similarly, define $\bar{F}(z) = F(z)z^{r_F}$ and $\tilde{F}(z) = \bar{F}(z)z^{-r_F+r_G}$, the H_2 norm of $T_{ed}(z)$ can be written as

$$\begin{aligned} \|F + GC_{ff}\|_2 &= \|\bar{F}z^{-r_F} + \bar{G}z^{-r_G}C_{ff}\|_2 \\ &= \|[\bar{F}z^{-r_F+r_G} + \bar{G}C_{ff}]z^{-r_G}\|_2 \\ &= \|\tilde{F} + \bar{G}C_{ff}\|_2. \end{aligned}$$

According to Lemma 1, we can conclude

$$\min_{C_{ff}(z)\in R\mathcal{H}_\infty} \|\tilde{F}(z) + \bar{G}(z)C_{ff}(z)\|_2 < \|\tilde{F}(z)\|_2$$

provided the following two conditions hold. First, $\tilde{F}(z)$ must be (strictly) proper, e.g. $r_F \geq r_G$. Second, $\bar{G}$ must have a feedthrough matrix D_G with $D_G^{\mathrm{T}} D_G > 0$. □

Theorem 1 states that the feedforward controller solved by the model matching method can improve the variance (H_2 norm) of the error signal e, provided 1) the relative degree of $F(z)$ is larger than or equal to that of $G(z)$ and 2) $G(z)z^{r_G}$ is well-posed. Furthermore, the larger the difference in the relative degrees of $F(z)$ and $G(z)$, the more we can reduce $\|F + GC_{ff}\|_2$. This is due to the fact that when the effective order of $\bar{F}(z)z^{-(r_F-r_G)}$ increases, a larger order $C_{ff}(z)$ with more controller parameters to minimize $\|F + GC\|_2$ is allowed. Adding extra delays in $F(z)$ can increase the difference between r_F and r_G.

2.4 Augmented Model Matching

Computing optimal feedforward controller by minimizing a norm on the transfer function $T_{ed}(z)$ may lead to a large control signal u_{ff}, as no penalty is imposed on the norm of $C_{ff}(z)$. In fact, the H_2 model matching in (2) becomes a minimum variance control problem without penalty on the control signal. This can be easily addressed by augmenting the model matching techniques in (2) with a simultaneous minimization of the (weighted) norm on $C_{ff}(z)$, as described in (6),

$$C_{ff}(z) = \arg \min_{C_{ff}(z)\in R\mathcal{H}_\infty} \left\| \begin{matrix} F(z) + G(z)C_{ff}(z) \\ C_{ff}(z)W(z) \end{matrix} \right\|_2, \quad (6)$$

where $W(z)$ is a stable discrete-time filter that acts as a weighting function for the feedforward control signal u_{ff}. The augmentation provides a trade-off between minimizing the variance of the output error e and the variance of the control signal u_{ff}. It is easily verified that the additional minimization of the variance of u_{ff} in (6) does not affect the results summarized in Theorem 1.

3 APPROXIMATE DYNAMIC INVERSION

Dynamic inversion is a commonly-used technique to design feedforward control for disturbance rejection. The presence of NMP zeros in the dynamics complicates the inversion as the NMP zeros become unstable poles in the inverse system. Denote the numerator and denominator of the plant transfer function $G(z)$ as $B_G(z)$ and $A_G(z)$, respectively. Denote the numerator as

$$B_G(z) = B_{sG}(z)B_{uG}(z),$$

where $B_{sG}(z)$ is the polynomial that contains all the zeros of $G(z)$ within the unit circle and $B_{uG}(z)$ is the polynomial of the NMP zeros, the plant dynamics then is

$$G(z) = \frac{B_{sG}(z)B_{uG}(z)}{A_G(z)}.$$

Approximate inversion techniques aim to seek an approximate inverse $\tilde{G}^{-1}(z)$ to solve the feedforward controller and

$$\tilde{G}^{-1}(z) = \frac{A_G(z)\tilde{B}_{uG}^{-1}(z)}{B_{sG}(z)},$$

where $\tilde{B}_{uG}^{-1}(z)$ is the approximate inverse of $B_{uG}(z)$. The goal is to find the approximate inverse of the NMP zero such that $G(z)\tilde{G}^{-1}(z) = B_{uG}(z)\tilde{B}_{uG}^{-1}(z) \approx 1$. We consider the simplest case where $G(z)$ contains only one NMP zero at $z = z_0$ ($|z_0| > 1$) and $B_{uG}(z) = z - z_0$.

3.1 Zero Phase Error Tracking Control

The Zero Phase Error Tracking Control (ZPETC) inversion method is introduced in [11]. This method approximates the inverse by reflecting the NMP zero in the original plant about the unit circle so as to cancel the phase shift due to the NMP zero, that is,

$$\tilde{B}_{uG}^{-1}(z) = \frac{1 - z_0 z}{(1 - z_0)^2}$$

and

$$\tilde{G}^{-1}(z) = \frac{A_G(z)(1 - z_0 z)}{B_{sG}(z)(1 - z_0)^2}.$$

Here, the gain $\frac{1}{(1-z_0)^2}$ is added to maintain unity DC gain of $G(z)\tilde{G}^{-1}(z)$. The resulting dynamic inverse is non-causal and an extra $k = r_G + 2$ steps of delay needs to be added so as to form a causal feedforward controller.

In general, a total number of $r_G + 2k_u$ steps of delay is needed, where k_u is the number of NMP zeros in the plant dynamics. The phase response of $G(z)\tilde{G}^{-1}(z)$ is zero at all frequency while the gain deviates from unity at higher frequency.

3.2 Zero Magnitude Error Tracking Control

In contrast to the ZPETC where the NMP zero is converted to a stable zero in the inverse system, the Zero Magnitude Error Tracking Control (ZMETC) reflects the NMP zero about the unit circle and coverts it to a stable pole in the inverse system [10]. Thus, the approximate inverse of $B_{uG}(z)$

$$\tilde{B}_{uG}^{-1}(z) = \frac{1}{(z_0 z - 1)}$$

and

$$\tilde{G}^{-1}(z) = \frac{A_G(z)}{B_{sG}(z)(z_0 z - 1)}.$$

To maintain the causality of the feedforward controller, an additional r_G steps of delay is needed. The product $G(z)\tilde{G}^{-1}(z)$ is

$$G(z)\tilde{G}^{-1}(z) = \frac{z - z_0}{z_0 z - 1}$$

and the magnitude response is always unity but there will be phase lag.

3.3 Non-causal Taylor Series Approximation

The non-causal Taylor series uses a non-causal, stable, Taylor series expansion to approximate the inverted unstable pole. Denote $p = \frac{z}{z_0}$ $(|p| < 1)$,

$$B_{uG}^{-1}(z) = \frac{1}{z - z_0} = -\frac{1}{z_0} \cdot (1 - p)^{-1}.$$

Using a $n_T{}^{th}$-order Taylor series to approximate $(1-p)^{-1}$, we have

$$\begin{aligned} \tilde{B}_{uG}^{-1}(z) &\approx -\frac{1}{z_0} \cdot \left(1 + p + p^2 + \cdots + p^{n_T}\right) \\ &= -\frac{1}{z_0} \cdot \frac{1 - p^{n_T}}{1 - p} \\ &= \frac{1 - (\frac{z}{z_0})^{n_T}}{z - z_0} \end{aligned}$$

and

$$\tilde{G}^{-1}(z) = \frac{A_G(z)}{B_{sG}(z)} \frac{1 - (\frac{z}{z_0})^{n_T}}{z - z_0}.$$

The resulting approximate inverse of $G(z)$ is a non-causal transfer function. A total number of $r_G + n_T$ extra steps of delay need to be added to the feedforward controller to make it causal. The magnitude of $G(z)\tilde{G}^{-1}(z)$ is closer to unity as n_T increases and $1 - (\frac{z}{z_0})^{n_T}$ gets closer to 1.

The feedforward controller designed using approximate dynamic inversion techniques are usually non-causal. Hence, the knowledge of the disturbance ahead of time is required to achieve good disturbance rejection performance. When the relative degree of the disturbance dynamics is higher than that of the plant dynamics (and so the model matching problem has a non-zero solution), the disturbance affects the feedforward path before the system output and the non-causal controller design is feasible. In practice, a feasible feedforward controller needs to be strictly proper and this leads to the requirements of a higher relative degree in $F(z)$.

4 SIMULATIONS

We employ the model matching method and the approximate dynamic inversion techniques on the head track-following servo system in a reel-to-reel tape system (Figure 2). The schematic is modified from the graphical user interface of a LTM simulation tool (LTMSim) [12].

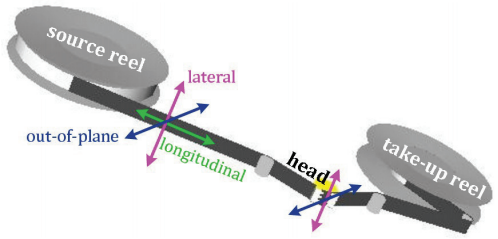

Figure 2: Schematic of tape head track-following system.

Data is recorded in tracks parallel to the edges of the tape and each data track spans the entire length of the tape. The contemporary tape is half inches wide and there are typically over a thousand tracks across the width of the tape. The tape winds longitudinally between the two reels and passes over the head, where data is read from or written to the tape. A voice coil actuator moves the head assembly laterally across the width of the tape to position the head on the desired track.

When tape transports longitudinally, it can exhibit lateral motion that misaligns the head and the desired track and increases position error. The typical peak-to-peak amplitude of measured lateral tape motion displacement (LTMD) data in an operating tape drive is about 10 μm [6] [7] [9]. Both the head and the tape can have out-of-plane motions that are beyond the scope of this paper. One primary purpose of the head positioning servo system is to follow the desired data track as accurately as possible during read/write operations in spite of disturbances such as the lateral tape motion. Feedforward control can be applied to reduce the effects of the LTM on the position error and improve the track-following performance of the head servo mechanism.

The tape head track-following system can be modeled as a spring-mass-damping system with a couple of resonances. A typical transfer function model from the voice coil motor current to the head position is

$$G(s) = \frac{K{\omega_1}^2{\omega_2}^2}{(s^2 + 2\zeta_1\omega_1 s + {\omega_1}^2)(s^2 + 2\zeta_2\omega_2 s + {\omega_2}^2)},$$

where ω_i $(i = 1, 2)$ are the two resonances and K is a gain. In this study, ω_1 is chosen to be 100 Hz and ω_2 is set to 1 KHz. The damping ratios are $\zeta_1 = 0.0796$ and $\zeta_2 = 0.05$ and the gain $K = 2000$. Using a zero-order hold (ZOH)

on all inputs as in [2], with a sampling rate of 10 KHz, the discrete-time transfer function is

$$G(z)=\frac{0.12633(z+9.52)(z+0.9853)(z+0.102)}{(z^2-1.986z+0.99)(z^2-1.569z+0.9391)}$$

and the Bode plot of the discrete-time model is depicted in Figure 3. The system is strictly proper with a relative degree $r_G = 1$. The NMP zero at -9.52 is due to the fast sampling rate [1].

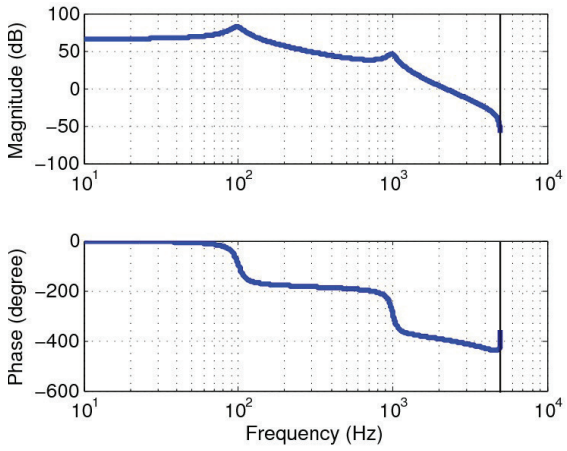

Figure 3: Bode plot of the tape head track-following model at a sampling frequency of 10 KHz.

In the simulation, the disturbance d is the lateral tape motion displacements near the head that are measured from an industry tape drive. Spectrum analysis shows the amplitude of d is on the order of 10 μm and the frequencies of the components are within 500 Hz. In the presented simulation results, the disturbance dynamics $F(z)$ is chosen to be a pure delay to better show the improvement in the disturbance rejection performance as the difference between the relative degrees of $F(z)$ and $G(z)$ increases. When $F(z)$ includes more dynamics, the same trend still holds but the overall disturbance rejection performance is not as good as when $F(z)$ is a pure delay.

4.1 Model Matching Methods

The *Matlab* robust control toolbox is used to solve for the optimal $C_{ff}(z)$ that simultaneously minimizes the H_2 norm of $T_{ed}(z)$ and the control input, as described in (6). A high-pass weighting filter $W(z)$ is used to limit the size of feedforward control input.

When $F(z)$ is a unity delay ($r_F = r_G = 1$), the solution of $C_{ff}(z)$ is simply zero. When $r_F - r_G = 2$, Figure 4 and 5 show the output error caused by the disturbance is reduced by 1 order of magnitude to the order of $10^{-1}\mu$m.

Increasing the steps of delay in $F(z)$ yields higher oder $C_{ff}(z)$ and better disturbance rejection performance. Figure 6 shows the output error is further reduced by 1 more order of magnitude to 10^{-2} μm when $r_F - r_G = 20$.

The maximum feedforward control input current is around 7 A and the RMS is about 0.9 A. Adjusting the

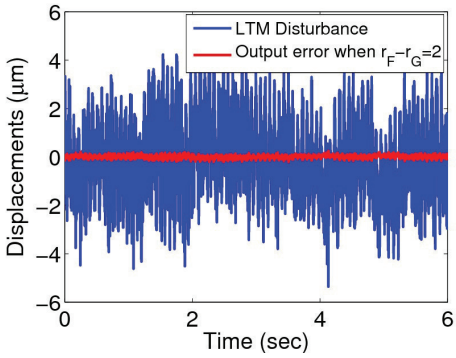

Figure 4: The feedforward controller designed by the H_2 norm model matching method reduces the position error when the difference between the relative degrees of $F(z)$ and $G(z)$ is 2.

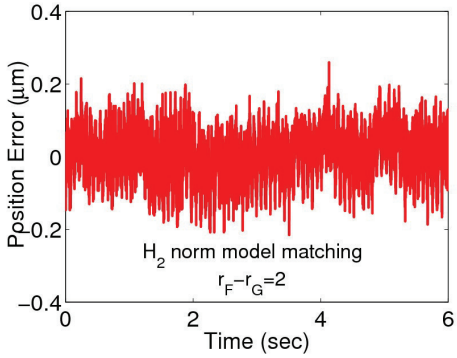

Figure 5: When the difference between the relative degrees of $F(z)$ and $G(z)$ is 2, the position error is reduced to 10^{-1} μm.

weighting function $W(z)$ to add more penalty to the control input can further constrain the size of the input at a cost of degrading the disturbance rejection performance. If the feedforward control input is allowed to be large, the model matching methods can achieve even better disturbance rejection performance.

4.2 Approximate Dynamic Inversion Techniques

The authors in [13] developed a number of feedforward controllers based on approximate dynamic inversion techniques to take into account the lateral tape motion (LTM) disturbances in the tape head positioning system. The approximate dynamic inversion techniques design $C_{ff}(z)$ independently on the disturbance dynamics $F(z)$. These controllers are non-causal and require as the input the knowledge of the disturbance in the future. In the simulations, delays are added in $F(z)$ as an alternative to obtaining knowledge of the disturbance ahead of time.

The disturbance rejection performance of the ZMETC and the ZPETC feedforward controller are similar for this application. We present the results of the ZMETC feedforward controller as it requires less additional delay than the ZPETC feedforward controller. When $F(z) = z^{-1}$, the disturbance is reduced by 1 order of magnitude as shown

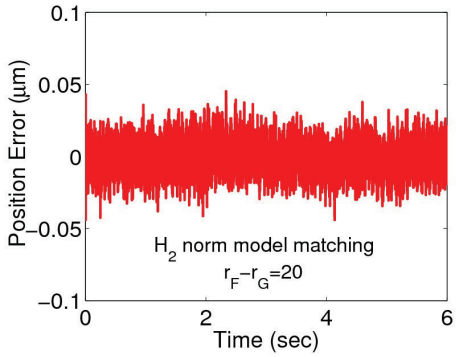

Figure 6: The error is further reduced to 10^{-2} μm when $F(z)$ is a 20-step delay.

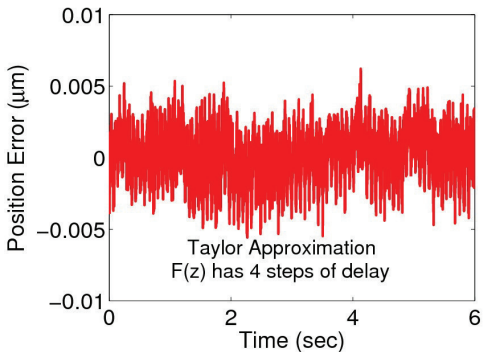

Figure 8: The position error is at $10^{-3}\mu$m when the feedforward controller is designed using the Taylor series approximation method.

in Figure 7. Figure 8 shows the simulated output error is reduced by 3 orders of magnitude when C_{ff} is designed using a third-order Taylor series approximation.

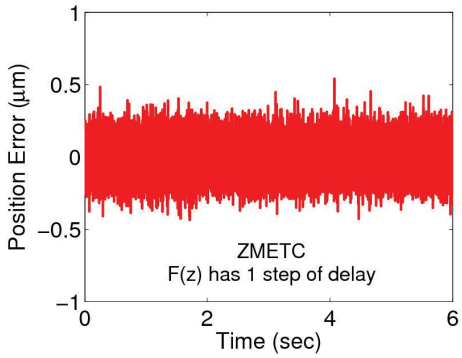

Figure 7: ZEMTC feedforward controller reduces the position error to $10^{-1}\mu$m.

In both simulations, the maximum value of the feedforward control input current is around 15 A and the RMS is about 3.5 A. The disturbance rejection performance will be degraded if the feedforward input is saturated.

5 CONCLUSIONS

This paper discusses model matching methods and approximate dynamic inversion techniques to design feedforward controllers for disturbance rejection. The model matching methods convert the disturbance rejection problem to an optimization problem in which the feedforward controller minimizes the norm of the transfer function from the disturbance to the output. Such an optimal controller can improve disturbance rejection only when the relative degree of the disturbance dynamics is higher than that of the plant dynamics. The approximate dynamic inversion techniques seek an approximate inverse of the plant to construct the feedforward controller. The resulting controllers are usually non-causal. If the disturbance dynamics have higher relative degree than the plant dynamics, the disturbance affects the feedforward path before it appears in the system output and a non-causal feedforward controller is acceptable. In the special case of minimum-phase systems, the model matching methods and the dynamic inversion techniques yield the same feedforward control design. These indicate some equivalence existing in these two different feedforward control design methods. We apply these methods to an example tape head track-following servo system in which the feedforward control is designed to reject the position error caused by the lateral tape motion disturbances. Simulation results demonstrate that the feedforward control effectively improves disturbance rejection performance of the servo system.

REFERENCES

[1] K. Åström, P. Hagander, and J. Sternby. Zeros of Sampled-data Systems. *Automatica*, vol. 20, no. 1, pp. 31-38, 1984.

[2] G. Franklin, J. Powell, and M. Workman. *Digital Control of Dynamic Systems*, Prentice Hall, 3rd edition, 1998.

[3] J. Doyle, B. Francis, and A. Tannenbaum. *Feedback Control Theory*, Macmillan, 1992.

[4] M. Green and D. Limebeer. *Linear Robust Control*, Prentice Hall, 1994.

[5] A. Hazell. Discrete-time Optimal Preview Control. *Ph.D. Thesis, Univ. of London*, 2008.

[6] Information Storage Industry Consortium (INSIC). International Magnetic Tape Storage Roadmap 2008. *INSIC, San Diego*, September 2008.

[7] V. Kartik. In-plane and Transverse Vibration of Axially-moving Media with Advanced Guiding and Actuation Elements, *Ph.D. Thesis, Carnegie Mellon University*, 2006.

[8] A. Oppenheim, A. Willsky, and S. Nawab. *Signals and Systems*, Prentice Hall, 2nd edition, 1996.

[9] B. Raeymaekers and F. Talke. Measurement and Sources of Lateral Tape Motion: A Review. *ASME J. Tribology-Transactions*, vol. 131, January 2009, pp. 65-68.

[10] B. Rigney. Adaptive Settle-Optimal Control of Servomechanisms. *Ph.D. Thesis, Univ. of Colorado Boulder*, 2008.

[11] M. Tomizuka. Zero Phase Error Tracking Algorithm for Digital Control. *ASME J. Dynamics, System, Measurement, and Control*, vol. 109, March 1987, pp. 1-6.

[12] J. Wickert and M. Brake. Tape Path Guiding Simulation Distribution. *INSIC Report*, October 2007.

[13] H. Zhong and L. Pao. Combined Feedforward/Feedback Control for Tape Head Track-Following Servo System. *Proceedings of IFAC World Congress 2011*, pp. 4040-4045.